Cinobufagin inhibits M2-like tumor-associated macrophage polarization to attenuate the invasion and migration of lung cancer cells

YING SUN[1], YUNFENG LIAN[1], XUE MEI[1], JINCHAN XIA[1], LONG FENG[1], JIANFENG GAO[1], HUAMING XU[1], XIAOYAN ZHANG[2], HUITONG YANG[1], XU HAO[1] and YILIN FENG[1]

[1]Department of Pathogenic Biology and Immunology, Medical College, Henan University of Chinese Medicine, Zhengzhou, Henan 450046, P.R. China; [2]Department of Epidemic Febrile Disease, Traditional Chinese Medical College, Henan University of Chinese Medicine, Zhengzhou, Henan 450046, P.R. China

Received April 3, 2024; Accepted August 14, 2024

DOI: 10.3892/ijo.2024.5690

Abstract. Macrophages have crucial roles in immune responses and tumor progression, exhibiting diverse phenotypes based on environmental cues. In the present study, the impact of cinobufagin (CB) on macrophage polarization and the consequences on tumor-associated behaviors were investigated. Morphological transformations of THP-1 cells into M0, M1 and M2 macrophages were observed, including distinct changes in the size, shape and adherence properties of these cells. CB treatment inhibited the viability of A549 and LLC cells in a concentration-dependent manner, with an IC_{50} of 28.8 and 30.12 ng/ml, respectively. CB at concentrations of <30 ng/ml had no impact on the viability of M0 macrophages and lung epithelial (BEAS-2B) cells. CB influenced the expression of macrophage surface markers, reducing CD206 positivity in M2 macrophages without affecting CD86 expression in M1 macrophages. CB also altered certain expression profiles at the mRNA level, notably downregulating macrophage receptor with collagenous structure (MARCO) expression in M2 macrophages and upregulating tumor necrosis factor-α and interleukin-1β in both M0 and M1 macrophages. Furthermore, ELISA analyses revealed that CB increased the levels of pro-inflammatory cytokines in M1 macrophages and reduced the levels of anti-inflammatory factors in M2 macrophages. CB treatment also attenuated the migration and invasion capacities of A549 and LLC cells stimulated by M2 macrophage-conditioned medium. Additionally, CB modulated peroxisome proliferator-activated receptor γ (PPARγ) and MARCO expression in M2 macrophages and epithelial-mesenchymal transition in A549 cells, which was partially reversed by rosiglitazone, a PPARγ agonist. Finally, CB and cisplatin treatments hindered tumor growth *in vivo*, with distinct impacts on animal body weight and macrophage marker expression in tumor tissues. In conclusion, the results of the present study demonstrated that CB exerted complex regulatory effects on macrophage polarization and tumor progression, suggesting its potential as a modulator of the tumor microenvironment and a therapeutic for cancer treatment.

Correspondence to: Professor Ying Sun, Department of Pathogenic Biology and Immunology, Medical College, Henan University of Chinese Medicine, 156 Jinshui East Road, Jinshui, Zhengzhou, Henan 450046, P.R. China
E-mail: sunying0109@163.com

Key words: macrophages, cinobufagin, polarization, lung cancer, peroxisome proliferator-activated receptor γ, tumor progression

Introduction

Lung cancer, a disease of notable global prevalence, carries substantial morbidity and mortality rates, posing a severe threat to human health (1-3). Annually, ~11.6% of newly diagnosed cancer cases and 18.4% of all cancer-related deaths are attributed to lung cancer (2,3). This disease is primarily categorized into small cell lung cancer and non-small cell lung cancer (NSCLC), with NSCLC comprising 80-85% of all lung cancer cases (4,5). Among these cases, >55% of patients with NSCLC are diagnosed with advanced cancer and have a poor prognosis (6,7). The conventional treatment regimen for NSCLC includes surgical resection of the primary tumor or metastatic lesions, radiotherapy and chemotherapy. However, resistance to a number of chemotherapy drugs, such as cisplatin (DDP), can develop, affecting patient outcomes (8,9). Although immunotherapy based on immune checkpoint inhibitors has been widely used clinically, only <25% of patients can achieve a durable immune response, possibly due to the immunosuppressive state of the tumor microenvironment (TME) (10-12). Therefore, improving the immunosuppressive state of the TME in patients with NSCLC and conceiving new treatment strategies have become urgent issues that need to be addressed.

Tumor invasion and metastasis are the results of the interaction and co-development between tumor cells and the TME (13). Macrophages in the TME are termed tumor-associated macrophages (TAMs) and are the main cells in the NSCLC microenvironment, not only enhancing

immune evasion of NSCLC as immunosuppressive cells but also directly participating in cancer progression (14-16). Studies have shown that in the initial stages of lung cancer formation, TAMs tend to be the M1 type, while during cancer invasion and migration, macrophages gradually polarize from M1 to M2 (14-16). Yuan *et al* (17) discovered that M2 macrophages promote A549 cell invasion and the growth of xenograft tumors, while M1 macrophages significantly reduce the expression of fibronectin and transforming growth factor-β (TGF-β), supporting tumor progression. M2 TAMs stimulate tumor cell invasion and migration, correlating with unfavorable outcomes in patients with NSCLC (18). Furthermore, TAMs foster an anti-inflammatory milieu and fuel tumor growth by releasing cytokines, chemokines, matrix metalloproteinases (MMPs), growth factors and other inflammatory agents (19). Notably, interleukin (IL)-10, platelet-derived growth factor and vascular endothelial growth factor (VEGF) have pivotal roles in NSCLC advancement (20). VEGF not only influences tumor migration and angiogenesis but fosters tumor progression through autocrine or paracrine signaling pathways (20). Upregulation of IL-10 in M2 TAMs is positively correlated with advanced NSCLC, possibly by affecting regulatory T lymphocytes to provide an immunosuppressive environment for tumor cells (21,22). Therefore, inhibiting macrophage polarization towards M2 and improving the balance of M1/M2 macrophages have become important strategies for NSCLC treatment.

Research has found that the activation of peroxisome proliferator-activated receptor γ (PPARγ) is a key factor in the polarization of M2 TAMs (23). PPARγ belongs to the nuclear receptor family and exerts anti-inflammatory effects (23), and is the main regulatory factor for adipocyte differentiation and function, favoring M2 phenotype activation (24). Research has found that arginase 1 (Arg-1) and macrophage galactose type C-type lectin-1 are direct target genes of PPARγ (25). In addition, the expression of PPARγ is induced by IL-13 and IL-4, both of which have been shown to induce M2 polarization (26). When macrophages are treated with PPARγ-specific agonists such as rosiglitazone (RSG), the secretion levels of pro-inflammatory factors are reduced (22). Therefore, PPARγ activation is crucial for M2 polarization.

HuaChanSu injection is a commonly used antitumor drug with significant clinical efficacy and is characterized by broad-spectrum anticancer activity, diverse clinical application modes and favorable tolerance in patients. In recent years, it has been widely used to treat various malignant tumors such as liver cancer, lung cancer, digestive tract malignant tumors, breast cancer and cervical cancer (27-29). A study has demonstrated that HuaChanSu injection combined with DDP significantly enhances efficacy in the treatment of advanced NSCLC, resulting in an improved patient quality of life and fewer adverse reactions (30). As the main active ingredient of HuaChanSu injection, cinobufagin (CB) is a bufadienolide steroid similar to digoxin, which also exerts antitumor activity (31). Research has found that CB can inhibit STAT3 phosphorylation and block the IL-6-induced nuclear translocation of STAT3, inhibiting epithelial-mesenchymal transition (EMT) of colorectal cancer (CRC) cells, thereby inhibiting the invasion and migration of CRC (32). In osteosarcoma, CB can enhance the transcription of the downstream genes of Forkhead Box Protein O1 (FOXO1), such as Fc fragment of IgG binding protein, regulating the expression of E-cadherin, transcription factor twist1, vimentin and MMP9 in ectopic implants, thereby inhibiting osteosarcoma progression (33). In NSCLC, CB inhibits A549 cell progression by upregulating FOXO1 and downregulating histone methyltransferase G9a (34). However, there is limited research on the inhibition of lung cancer progression by CB, and its specific mechanism of action requires further validation. Therefore, based on the notable clinical antitumor efficacy of HuaChanSu injection (29), the present study aimed to reveal the influence and mechanism of action of its effective active ingredient, CB, on the polarization of TAMs and on NSCLC progression, to provide a theoretical basis for further exploring the pharmacological effects and clinical applications of CB.

Materials and methods

Cell lines. The THP-1 human monocytic leukemia cell line (cat. no. FH0112) was procured from Shanghai Fuheng Biotechnology Co., Ltd., while the A549 human lung adenocarcinoma cell line (cat. no. CCL-185), LLC (cat. no. CRL-1642) and BEAS-2B human normal lung epithelial cells (cat. no. CRL-3588), human umbilical vein endothelial cells (HUVECs; cat. no. CRL-1730) were obtained from the American Type Culture Collection. Upon revival, the THP-1, BEAS-2B, A549 HUVEC and LLC cells were cultured in RPMI-1640 medium (Beijing Solarbio Science & Technology Co., Ltd.) supplemented with 10% fetal bovine serum (FBS; cat. no. 164210; Wuhan PuNuoSai Biotech Co., Ltd.) and maintained in a 37˚C and 5% CO_2 incubator. Upon reaching 80-90% confluency, adherent cells were detached using 0.25% EDTA-trypsin or directly pipetted, while suspended cells were collected by centrifugation at 4˚C and 1,200 x g for 5 min. Cells in the logarithmic growth phase were utilized for subsequent experiments.

Establishment of M1/M2 macrophage models. The establishment of M1/M2 macrophage models was performed according to previous studies (35,36). THP-1 cells into M0 macrophages were induced using the widely employed phorbol 12-myristate 13-acetate (PMA; cat. no. P1585; Sigma-Aldrich; Merck KGaA), which was followed by polarization into the M1 or M2 macrophage phenotypes using interferon-γ (IFN-γ) or IL-4 (PeproTech China), respectively. For the generation of M0 macrophages, THP-1 cells in the logarithmic growth phase were centrifuged at 4˚C and 1,200 x g for 5 min, the supernatant was aspirated and the cells were resuspended in RPMI-1640 medium supplemented with PMA (200 ng/ml) for 24 h. Subsequently, the cell concentration was adjusted to $1x10^6$ cells/ml before seeding into a 6-well plate. For the generation of M1 macrophages, the M0 macrophages were incubated in RPMI-1640 complete medium supplemented with a IFN-γ (20 ng/ml) for 24 h. Similarly, to induce the generation of M2 macrophages, M0 macrophages were cultured in RPMI-1640 complete medium supplemented with IL-4 (20 ng/ml) for 24 h.

Preparation of conditioned medium. Culture medium from the 6-well plate containing macrophages in various polarization states was aspirated, and the plate was washed twice with

phosphate-buffered saline (PBS). Subsequently, the macrophages were incubated in serum-free RPMI-1640 medium at 37˚C with 5% CO_2 for 24 h. Following this incubation period, the culture medium was harvested in a 5-ml sterile Eppendorf tube and centrifuged at 4˚C and 13,800 x g for 15 min. The resulting supernatant, designated as the conditioned medium, was carefully transferred to another 5-ml sterile Eppendorf tube and stored at -80˚C for future use.

Treatments. For the CB treatment, macrophages were exposed to various concentrations of CB (Sigma-Aldrich; Merck KGaA; 10, 15, 20, 25, 30, 35, 40 and 50 ng/ml) for 24 h before being prepared for subsequent experiments. Similarly, for RSG treatment, macrophages were exposed to various concentrations of RSG (Sigma-Aldrich; Merck KGaA; 0.1, 0.5, 1, 5 and 10 μM) for 24 h before being prepared for further experiments. In certain investigations, macrophages were exposed to conditioned medium from M0, M1 or M2 macrophages for 24 h.

MTT assay. M0 macrophages and BEAS-2B, A549 and LLC cells were prepared as single-cell suspensions. After counting, the cells were seeded into a 96-well culture plate at a density of $1x10^4$ cells in 200 μl of medium per well, with 6 replicate wells per group. The next day, after cell adherence, various concentrations of CB or RSG were added to the wells for intervention, in which the control group was treated with an equivalent dose of DMSO (not exceeding 0.1% of the maximum dose). Following a 24-h incubation, 20 μl of 5 mg/ml MTT solution (Beijing Solarbio Science & Technology Co., Ltd.) was added to each well, and the plate was further incubated for ~4 h. Subsequently, 150 μl DMSO solution was added to each well and was used to dissolve the purple formazan, and the plate was shaken at room temperature for 15-20 min. The absorbance (A) values of each well were measured at 490 nm, with blank wells set to 0. The cell viability was then calculated using the following formula: Cell viability (%)=(experimental group A value/control group A value) x100%.

Flow cytometry. The culture medium from the 6-well plate containing macrophages in different polarization states was aspirated. The plate was then washed with PBS, which was repeated twice. The cells were scraped off using a cell scraper, repeating this step twice, and collected in a centrifuge tube. The collected cells were gently pipetted repeatedly and then centrifuged at 1,200 x g for 5 min at room temperature. After centrifugation, the cells were resuspended in PBS at a final concentration of $1x10^5$ cells/ml, then non-specific antigens were blocked using 5% BSA buffer (MilliporeSigma) for 20 min at room temperature. For intracellular CD86 staining, fixation in 4% paraformaldehyde for 20 min at room temperature and permeabilization with 0.1% Triton X-100 were performed prior to staining. The cells were then stained with monoclonal mouse anti-human CD86 (1:50; cat. no. PE-65155) and CD206 (1:100; cat. no. FITC-65165) antibodies (both from Proteintech Group, Inc.) for 30 min at 4ºC in the dark. Subsequently, the cells were analyzed using a BD FACSCanto II flow cytometer (BD Biosciences) and the FlowJo 10 software (BD Biosciences). A non-specific mouse Ig was used as an isotype control.

Table I. Sequences of primers used for reverse transcription-quantitative PCR.

Gene name	Primer sequence (5'-3')
CD68	F: GGAAATGCCACGGTTCATCCA
	R: TGGGGTTCAGTACAGAGATGC
CD206	F: CTACAAGGGATCGGGTTTATGGA
	R: TTGGCATTGCCTAGTAGCGTA
IL-10	F: GGTTGCCAAGCCTTGTCTGA
	R: AGGGAGTTCACATGCGCCT
MARCO	F: CAGCGGGTAGACAACTTCACT
	R: TTGCTCCATCTCGTCCCATAG
Arg-1	F: CTGTGGGAAAAGCAAGCGAG
	R: CATGGCCAGAGATGCTTCCA
TNF-α	F: CCTCTCTCTAATCAGCCCTCTG
	R: GAGGACCTGGGAGTAGATGAG
IL-1β	F: ATGATGGCTTATTACAGTGGCAA
	R: GTCGGAGATTCGTAGCTGGA
IL-6	F: ACTCACCTCTTCAGAACGAATTG
	R: CCATCTTTGGAAGGTTCAGGTTG
PPARγ	F: TTCAGAAATGCCTTGCAGTG
	R: GGGGGTGATGTGTTTGAACT
GAPDH	F: TCCAAAATCAAGTGGGGCGA
	R: AGTAGAGGCAGGGATGATGT

F, forward; R, reverse; PPARγ, peroxisome proliferator-activated receptor γ; MARCO, macrophage receptor with collagenous structure.

Reverse transcription-quantitative PCR (RT-qPCR). Total RNA in cells was extracted using the TRIzol method (Thermo Fisher Scientific, Inc.). The total RNA concentration of each sample was measured using a NanoDrop-2000 UV spectrophotometer. RT was performed using the RevertAid First Strand cDNA Synthesis Kit (cat. no. K1621; Thermo Fisher Scientific, Inc.) according to the manufacturer's protocol and qPCR was conducted using the PowerUp™ SYBR™ Green Master Mix (cat. no. A25743; Thermo Fisher Scientific, Inc.). PCR thermocycling conditions were as follows: Denaturation at 94˚C for 120 sec, followed by 40 cycles consisting of melting (95˚C; 15 sec) and annealing/extension (60˚C; 60 sec) phases. GAPDH was used as an internal reference to calculate the relative transcription level of the target gene by the $2^{-\Delta\Delta Cq}$ method (37). The primer sequences are shown in Table I.

Immunofluorescence (IF). Cells were seeded at a density of $5x10^5$ cells/ml in confocal culture dishes to prepare macrophages in different states. The culture medium was removed and the wells were washed twice with PBS. Next, 500 μl of 4% paraformaldehyde was added to each well and incubated at room temperature for 30 min, then 500 μl of 0.5% Triton X-100 was added to each well and further incubated at room temperature for 10 min. Blocking solution was next added to the wells and incubated at room temperature for 15 min. Then, primary antibodies against PPARγ (1:350; cat. no. 66936-1-Ig; Proteintech Group, Inc.) and macrophage receptor with collagenous structure (MARCO; 1:400; cat. no. bs-2659R; BIOSS)

were added to each well and incubated overnight at 4˚C. The next day, the corresponding fluorescent secondary antibody (1:200; cat. no. A23210, Abbkine Scientific Co., Ltd.) was added to the wells and incubated at room temperature for 1 h. DAPI (10 μg/ml) staining was performed for 5 min at room temperature in the dark, followed by imaging using a laser confocal microscope.

ELISA. protein levels of tumor necrosis factor (TNF)-α (cat. no. E-EL-H0109c; Elabscience Biotechnology Co., Ltd.), IL-6 (cat. no. E-EL-H0102c; Elabscience Biotechnology Co., Ltd.), IL-1β (cat. no. E-EL-H0149c; Elabscience Biotechnology Co., Ltd.), TGF-β (cat. no. MM-1774H1; Jiangsu Meimian Industrial Co., Ltd.) and IL-10 (cat. no. MM-0066H1; Jiangsu Meimian Industrial Co., Ltd.) were determined by respective ELISA assay kits.

Wound healing. Cells were seeded into a 6-well plate at a density of $8x10^5$ cells/ml. The macrophage-conditioned medium was thawed and mixed with RPMI-1640 medium with 1% FBS. After the cells had adhered to the plate and the cell confluency was >90%, a vertical scratch was made in the center of each well using a 200 μl pipette tip. The culture medium was then removed, the scratched cells were washed with sterile PBS to remove non-adherent cells and fresh mixed culture medium was added to the plate. The 6-well plate was placed horizontally in a 5% CO_2 and 37˚C incubator. After 24 h, images were collected under a light microscope, and the results were measured and analyzed using ImageJ software version 1.48 (National Institutes of Health). Wound healing rate=(0 h scratch width-24 h scratch width)/0 h scratch width x100%.

Cell invasion. The cell invasion assay was performed using a 6-well 8-μm Transwell chamber. For this, Matrigel was diluted with ice-cooled serum-free medium, and 150 μl of the matrix gel was added to each well. The 6-well plate was then placed in a cell culture incubator at 37˚C with 5% CO_2 for 30 min. The 6-well plate was then placed in a cell culture incubator with 5% CO_2 at 37˚C for 30 min. Next, 2 ml A549 or LLC cell suspension ($5x10^5$ cells/ml) was added to the upper chamber, and 2 ml macrophage-conditioned medium was added to the lower chamber. After incubation for 48 h, the cells in the upper chamber were wiped off with a cotton swab, and the invasive cells were fixed with 4% paraformaldehyde at room temperature for 30 min, washed with PBS, stained with 0.1% crystal violet solution for 30 min at room temperature, and then observed and imaged under a light microscope. Cell counting was subsequently performed using ImageJ.

Western blotting. The culture medium was aspirated and the wells were washed twice with PBS. The 6-well plate was then transferred onto ice and 250 μl pre-prepared RIPA lysis buffer (cat. no. R0010; Beijing Solarbio Science & Technology Co., Ltd.) containing protease and phosphatase inhibitors (cat. no. P0100; Beijing Solarbio Science & Technology Co., Ltd.) was added to each well. The plate was further cooled on ice and the cells lysed for 30 min. The lysate was then transferred to a 1.5-ml sterile Eppendorf tube and centrifuged at 4˚C and 13,800 g for 15 min. The protein concentration was determined using the BCA method and the proteins were then denatured. Subsequently, protein samples (50 μg for each lane) were separated on 10% SDS-polyacrylamide gels, followed by transferring onto PVDF membranes (MilliporeSigma). The PVDF membranes were blocked with 5% BSA (MilliporeSigma) for 2 h at room temperature. After that, primary antibodies against Arg-1 (1:1,000; cat. no. bs-23837R; BIOSS), inducible nitric oxide synthase (iNOS; 1:1,000; cat. no. bs-0162R; BIOSS); phosphorylated (p)-PPARγ (1:1,000; cat. no. bs-3737R; BIOSS), vimentin (1:1,000; cat. no. bsm-33170M; BIOSS), E-cadherin (1:1,000; cat. no. bs-1519R; BIOSS), N-cadherin (1:1,000; cat. no. bs-20623R; BIOSS) and GAPDH (1:3,000; cat. no. 60004-1-Ig; Proteintech Group, Inc.) were incubated with the membrane overnight at 4˚C, followed by washing with Tris-buffered saline containing 0.05% Tween 20 and incubation with horseradish peroxidase-conjugated secondary antibodies goat anti-mouse IgG (1:10,000; cat. no. SA00001-1) and goat anti-rabbit IgG (1:10,000; SA00001-2; both from Proteintech Group, Inc.) at room temperature for 1 h. The western blot bands were visualized using an ECL kit (cat. no. PE0010; Beijing Solarbio Science & Technology Co., Ltd.). Densitometric analysis was performed using ImageJ software version 1.48 (National Institutes of Health).

Tube formation assay. For the preparation of conditioned medium, macrophages were treated with the aforementioned drugs, the drug-containing supernatant was removed and the cells were cultured for 24 h. The supernatant was then collected as conditioned medium for culturing cancer cells (A549 and LLC) for 24 h. After removing the supernatant, fresh culture medium was added to the cancer cells and the culturing was continued for another 24 h. The supernatant was then collected as conditioned medium for culturing HUVECs for 24 h. Matrigel Basement Membrane Matrix (BD Biosciences) was diluted with EBM-2 medium (Thermo Fisher Scientific, Inc.) and used to coat 24-well plates at 37˚C for 1 h. Subsequently, $5x10^4$ HUVECs were treated with different conditioned media from the A549 or LLC cells for 24 h. The tube formation ability of HUVECs was then assessed by quantifying the number of meshes, tube length and number of branches.

In vivo tumor growth. All animal studies were conducted following protocols approved by the Animal Ethics Committee of Henan University of Chinese Medicine (Zhengzhou, China; approval no. IACUC-202302006). In this experiment, 18 6-8-week-old male BALB/c nude mice (18-21 g) were randomly assigned to 3 groups (n=6 per group) and housed in standard cages at 20-24˚C with a 12/12-h light-dark cycle and *ad libitum* access to food and water. A 100-μl PBS suspension containing $5x10^6$ LLC cells was subcutaneously injected into the right flank of each mouse. To assess the effect of the LLC cells, data were collected every 5 days starting 4-5 days after tumor cell inoculation, which included animal weight and tumor dimension measurements. The mice were continuously fed for 25 days and received intraperitoneal injections of CB (10 mg/kg/day) (38,39) or DDP (2 mg/kg/day). For subcutaneous tumors, the maximum allowable diameter was 20 mm for each mouse. The tumor size was checked every other 1-2 days. The biggest tumor volume in the present study was 2,664.12 mm^3. At the end of the experiments, the mice were euthanized using

CO_2 (30-70% volume displacement of the chamber air per min) followed by cervical dislocation as a secondary method of euthanasia, in accordance with the approved protocol of the Experimental Animal Ethics Committee. The tumors from all animals were collected for subsequent analysis.

Statistical analysis. Experimental data were analyzed using GraphPad Prism 8.0 (Dotmatics) statistical software and are presented as the mean ± standard deviation. Normal distribution of the data was assessed by the Kolmogorov-Smirnov test. The unpaired Student's t-test was used for the comparison of differences between two groups, and one-way ANOVA followed by Bonferroni's multiple comparison tests was used for the comparison of differences among >2 groups. $P<0.05$ was considered to indicate a statistically significant difference.

Results

Morphology of the THP-1 cells and M0, M1 and M2 macrophages. The THP-1 cells appeared round and proliferated in suspension. Following induction with PMA for 24 h, the THP-1 cells underwent differentiation into M0 macrophages, which was accompanied by observable morphological changes. These changes included an increase in cell volume, resulting in an oval-shaped appearance, with a few fibroblast-like pseudopodia extending from the periphery. The cells also began to adhere to a surface. Upon the subsequent induction with IFN-γ, the M1 macrophages exhibited further changes, including an increased volume, enhanced surface adherence and an elongated morphology. Conversely, upon induction with IL-4, the M2 macrophages displayed an increase in volume, maintained an oval-shaped morphology, exhibited extending pseudopodia and tended to aggregate for growth (Fig. 1).

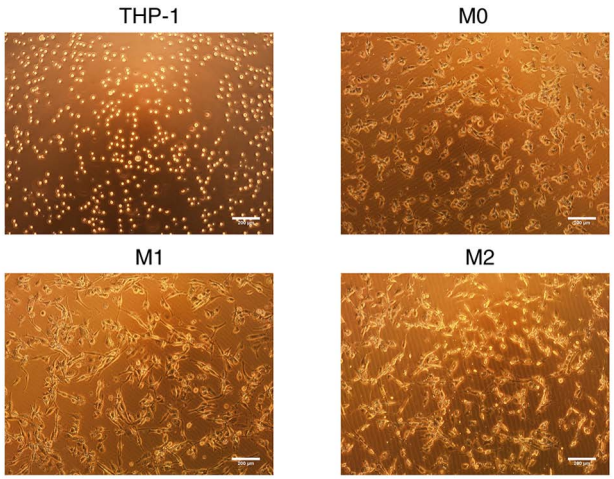

Figure 1. Morphology of the THP-1, M0, M1 and M2 macrophages as determined by light microscopy.

Effects of CB on the viability of M0 macrophages, BEAS-2B cells and lung cancer cells. The M0 macrophages were exposed to varying concentrations of CB, resulting in a concentration-dependent decrease in cell viability (Fig. 2A). Similarly, treatment with CB for 24 h resulted in a decrease in normal lung epithelial cell (BEAS-2B) viability starting at a concentration of 30 ng/ml (Fig. 2B). Additionally, CB exhibited a concentration-dependent reduction in the viability of A549 and LLC cells, with a calculated IC_{50} of 28.80 and 30.12 ng/ml, respectively (Fig. 2C and D). CB treatment inhibited the viability of A549 and LLC cells in a concentration-dependent manner, while concentrations below 30 ng/ml had no impact on the viability of M0 macrophages and BEAS-2B lung epithelial cells.

Effect of CB on macrophage surface markers under different polarization states. THP-1 monocytes differentiate into macrophages when induced by PMA, leading to changes in cell morphology and surface markers (40). Therefore, macrophage surface markers were assessed using flow cytometry in the present study. The findings revealed a higher percentage of $CD86^+$ cells in M1 macrophages compared with M0 macrophages, and CB treatment did not influence the percentage of $CD86^+$ cells in the M1 macrophages (Fig. 3A and B). Furthermore, the percentage of $CD206^+$ cells was higher in M2 macrophages compared with M0 macrophages. Nevertheless, CB treatment significantly reduced the percentage of $CD206^+$ cells in the M2 macrophages (Fig. 3C and D). The findings indicated that THP-1 monocytes, upon differentiation into macrophages via PMA induction, exhibit specific changes in surface markers.

Effect of CB on the mRNA expression of macrophage-related factors in different polarization states. The RT-qPCR results revealed significantly higher levels of CD206, Arg-1 and PPARγ mRNA expression in M2 macrophages compared with M0 macrophages (Fig. 4A-C). CB treatment failed to affect the CD206 and PPARγ levels in M0 macrophages, while Arg-1 mRNA expression was upregulated in the M0 + CB group compared with the M0 group (Fig. 4A-C). Notably, CB treatment led to a significant downregulation of MARCO mRNA expression in M2 macrophages (Fig. 4D). Consistent findings regarding the protein expression levels of Arg-1, PPARγ and MARCO were detected by western blotting (Fig. S1). Additionally, the TNF-α and IL-1β mRNA expression levels were upregulated in M1 macrophages compared with M0 macrophages. Furthermore, CB treatment significantly increased TNF-α and IL-1β mRNA expression in M0/M1 macrophages (Fig. 4E and F). These results indicated that M2 macrophages had elevated CD206, Arg-1 and PPARγ mRNA levels, which were unaffected by CB in M0 macrophages (except Arg-1 upregulation), while CB downregulated MARCO in M2 macrophages and increased TNF-α and IL-1β mRNA in both M0 and M1 macrophages.

Effect of CB on the protein levels of macrophage-related factors in different polarization states. Supernatant proteins were assessed using ELISA. There was a significant increase in the IL-6, IL-1β and TNF-α protein levels in the supernatant of M1 macrophages compared with M0 macrophages (Fig. 5A-C). Upon CB treatment, there was a further augmentation in IL-6, IL-1β and TNF-α protein levels in the supernatant of M1 macrophages (Fig. 5A-C). Additionally, the IL-10 and TGF-β levels were higher in the supernatant of M2 macrophages compared with M0 macrophages. However, CB treatment resulted in a reduction in IL-10 and TGF-β protein

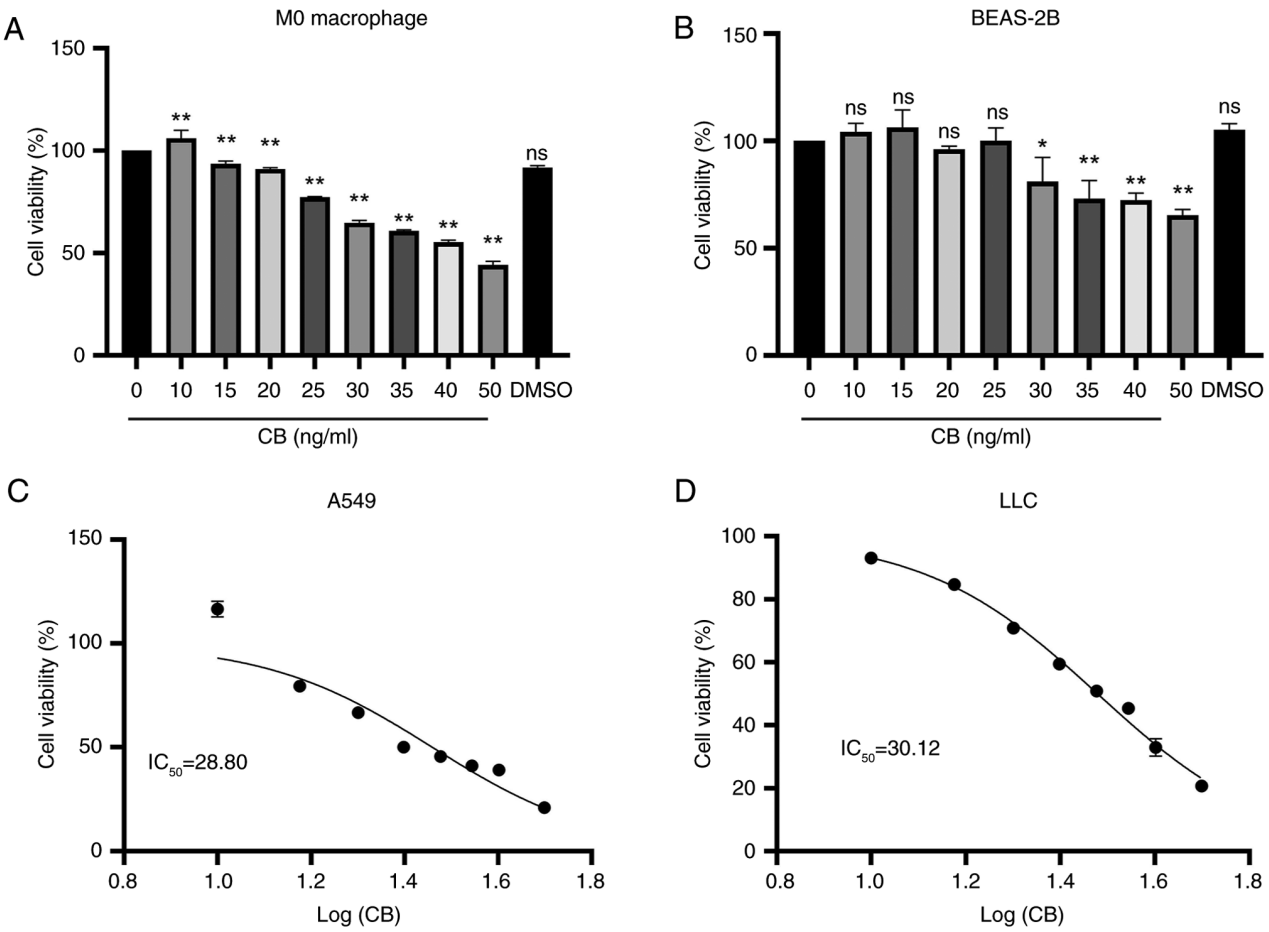

Figure 2. Effects of CB on the cell viability of M0 macrophage and BEAS-2B cells. (A) M0 macrophages and (B) BEAS-2B cells were treated with different concentrations of CB for 24 h; cell viability was detected by MTT assay. (C) A549 cells and (D) LLC cells were treated with different concentrations of CB; cell viability was detected by MTT assay (n=3). *P<0.05 and **P<0.01 compared with control group (0 ng/ml CB). CB, cinobufagin; ns, not statistically significant compared with 0 ng/ml CB group.

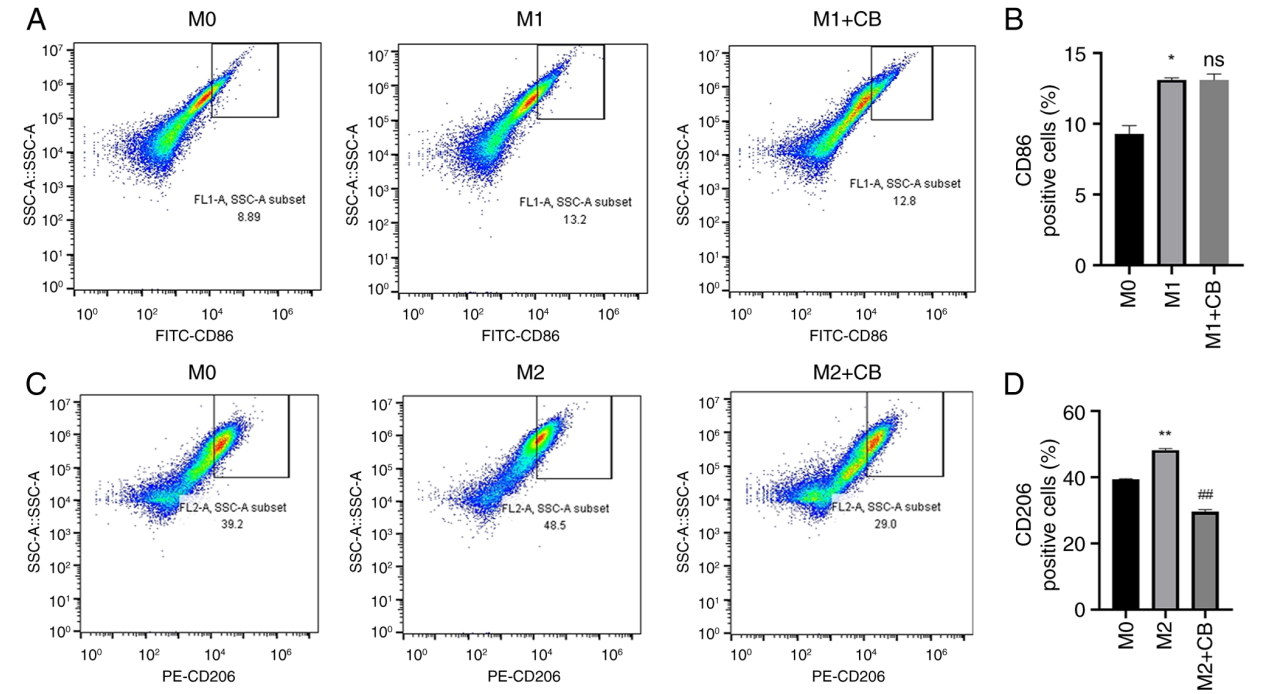

Figure 3. Effect of CB on the expression of macrophage surface markers under different polarization states. (A and B) Flow cytometry was used to quantify the expression of CD86, an M1 marker. (C and D) Flow cytometry was used to quantify the expression of CD206, an M2 macrophage marker (n=3). *P<0.05 and **P<0.01 compared with M0 group; $^{\#\#}$P<0.01 compared with M2 group. CB, cinobufagin; ns, not statistically significant compared with M1 group.

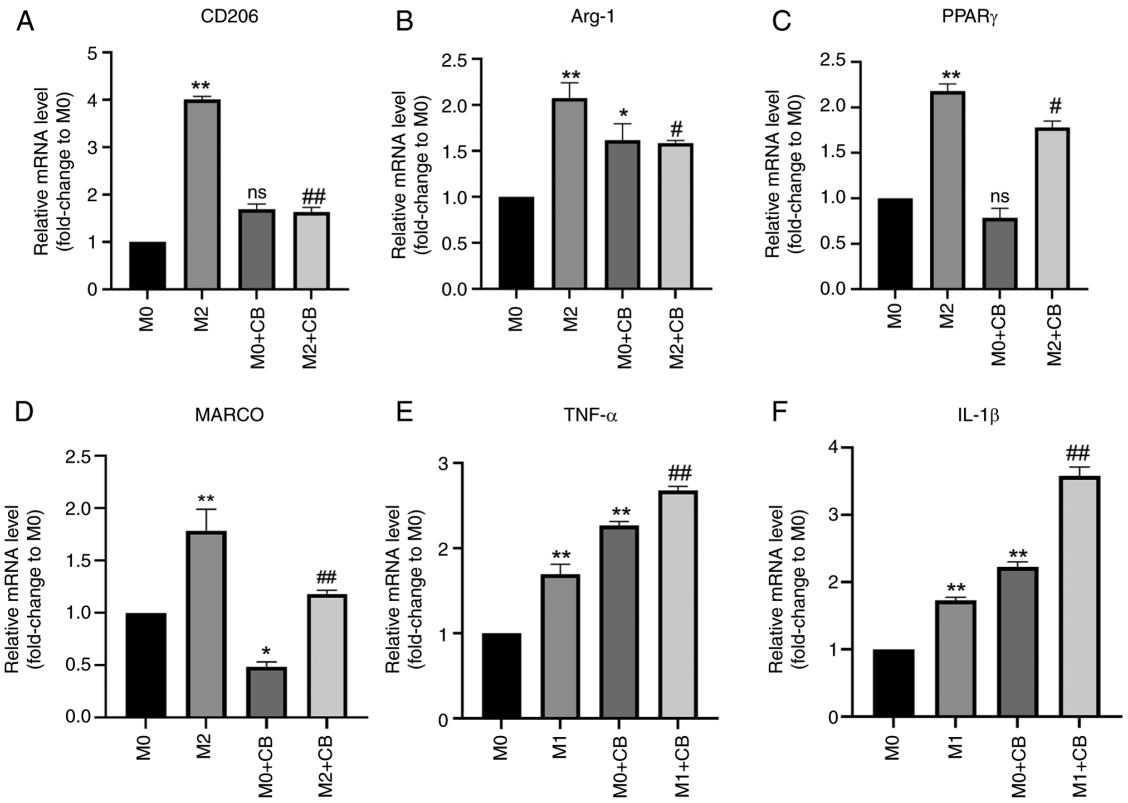

Figure 4. Effect of CB on mRNA expression of macrophage related factors in different polarization states. (A-F) The mRNA expression of (A) CD206, (B) Arg-1, (C) PPARγ, (D) MARCO, (E) TNF-α and (F) IL-1β in the macrophages with different treatments was determined by reverse transcription-quantitative PCR (n=3). *P<0.05 and **P<0.01 compared with M0 group; $^{\#}$P<0.05 and $^{\#\#}$P<0.01 compared with M2 group. CB, cinobufagin; Arg-1, arginase 1; PPARγ, peroxisome proliferator-activated receptor γ; MARCO, macrophage receptor with collagenous structure.

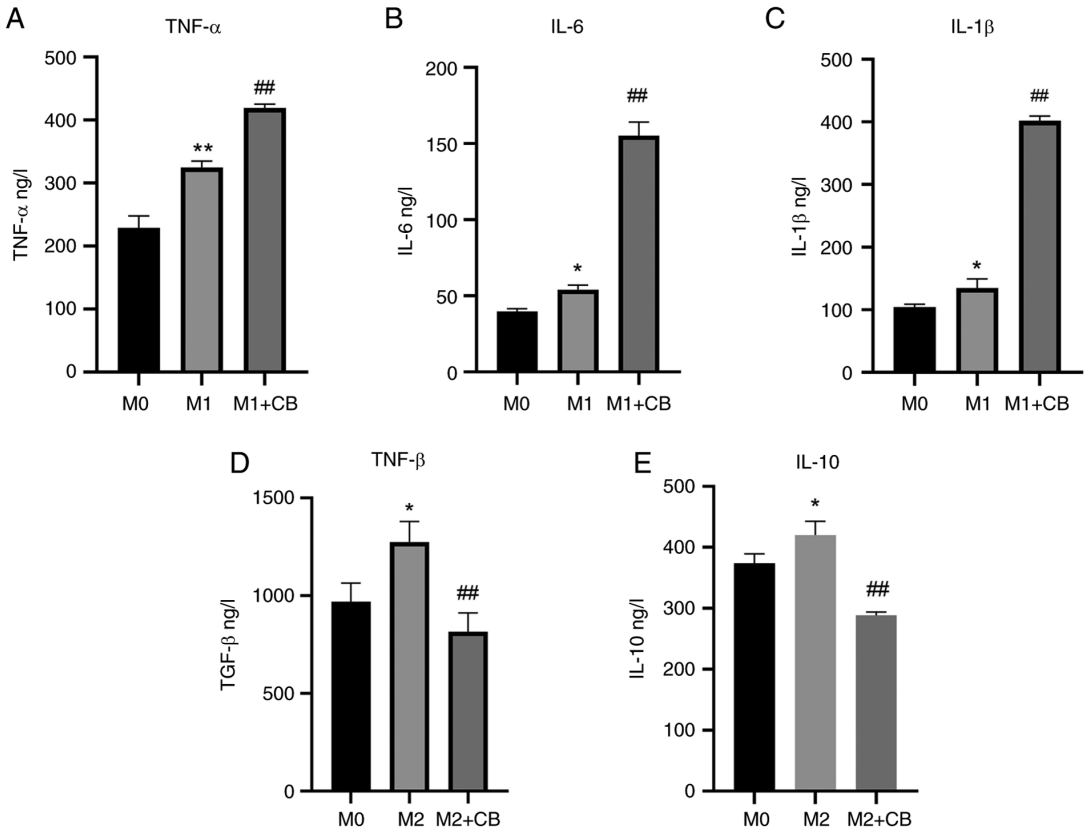

Figure 5. Effect of CB on protein levels of macrophage related factors in different polarization states. (A-E) The protein levels of (A) TNF-α, (B) IL-6, (C) IL-1β, (D) TGF-β and (E) IL-10 in different groups were determined by ELISA assay (n=3). *P<0.05 and **P<0.01 compared with M0 group; $^{\#\#}$P<0.01 compared with M1 or M2 group. CB, cinobufagin.

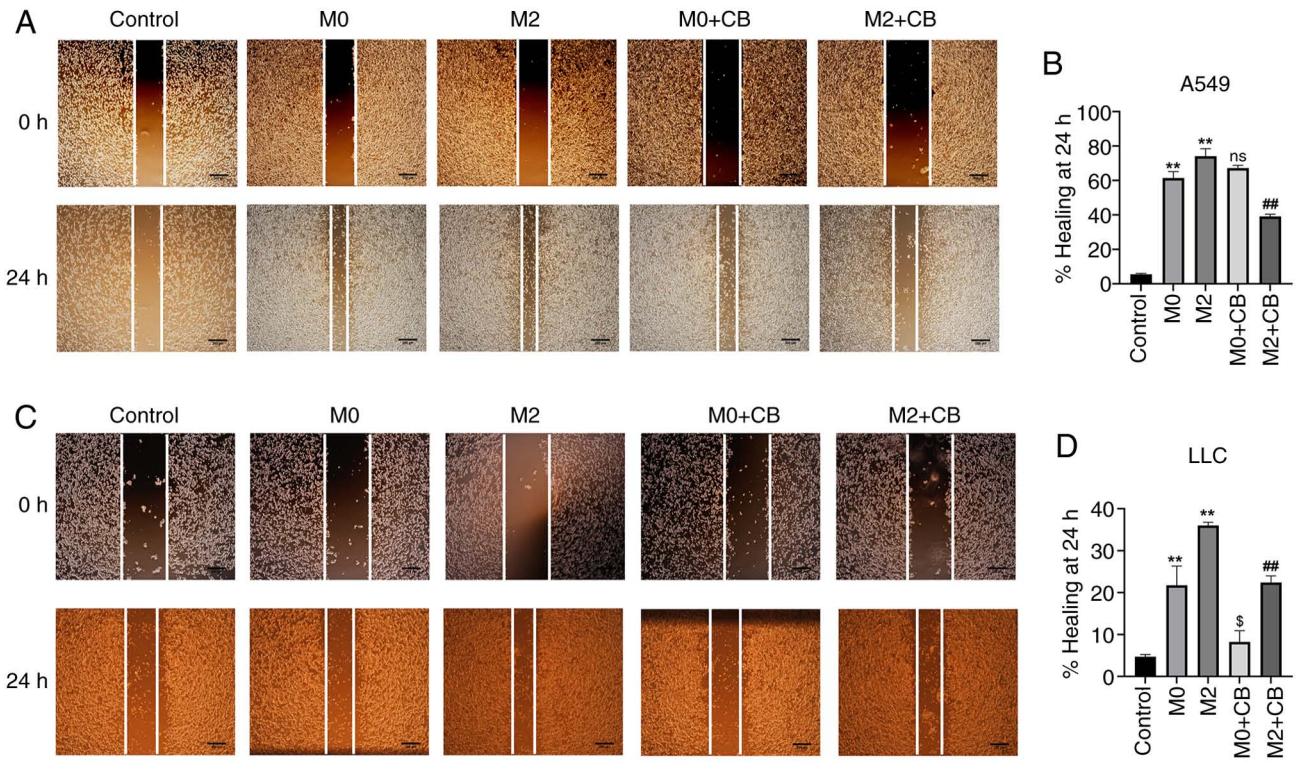

Figure 6. Effect of CB on migration of A549 and LLC cells on conditioned medium culture of macrophages in different polarization states. (A and B) Migratory ability of A549 cells with different treatments as evaluated by wound healing assay. (C and D) Migratory ability of LLC cells with different treatments was evaluated by wound healing assay (n=3). **P<0.01 compared with M0 group; $^{\#\#}$P<0.01 compared with M2 group; $^{\$}$P<0.05 compared with M0 group. CB, cinobufagin; ns, not statistically significant compared with M0 group.

levels in the supernatant of M2 macrophages (Fig. 5D and E). The results indicated that IL-6, IL-1β and TNF-α levels were elevated in M1 macrophages and further increased with CB treatment, while IL-10 and TGF-β levels were higher in M2 macrophages but decreased with CB treatment.

Effect of CB-treated macrophage-conditioned medium on the migration of A549 and LLC cells. In the complex TME, TAMs interact with the TME, undergo metabolic changes and alter the anticancer phenotype of early M1-TAMs (38). Typically, in the early stages of tumor development, M1-like TAMs predominate the TME and inhibit tumor growth by secreting certain inflammatory factors (39). As cancer progresses, late-stage M2-like TAMs begin to dominate the TME, promoting angiogenesis and aiding tumor cell dissemination and metastasis, thus exhibiting pro-tumor effects (40). In the present study, M0 macrophage-conditioned medium treatment significantly improved the wound healing of A549 and LLC cells compared with the control group (Fig. 6A-D). Additionally, M2 macrophage-conditioned medium further enhanced the migratory abilities of A549 and LLC cells compared with the M0 group (Fig. 6A-D). However, CB-treated M0 macrophage-conditioned medium showed no significant effect on the migration of A549, but attenuated the migration of LLC cells compared with the M0 group (Fig. 6A-D). Furthermore, CB-treated M2 macrophage-conditioned medium reduced A549 and LLC cell migration compared with the M2 group (Fig. 6A-D). The results indicated that M0 macrophage-conditioned medium significantly enhanced wound healing in A549 and LLC cells, with M2 macrophage-conditioned medium further boosting their migratory abilities, while CB-treated M0 medium had no significant effect on A549 migration but reduced LLC migration, and CB-treated M2 medium decreased migration in both cell types.

Effect of CB-treated macrophage-conditioned medium on A549 and LLC cell invasion. M2 macrophage-conditioned medium enhanced A549 and LLC cell invasion compared with the M0 group (Fig. 7A-D). However, CB-treated M0 macrophage-conditioned medium showed no significant effect on A549 and LLC cell invasion compared with the M0 group (Fig. 6A-D). Furthermore, CB-treated M2 macrophage-conditioned medium reduced A549 and LLC cell invasion compared with the M2 group (Fig. 7A-D). These results indicated that M2 macrophage-conditioned medium enhanced A549 and LLC cell invasion, whereas CB treatment had no significant effect on M0 macrophage-conditioned medium but reduced invasion in CB-treated M2 macrophage-conditioned medium.

Effects of conditioned medium from lung cancer cells treated with macrophage-conditioned medium on angiogenesis. First, lung cancer cells (A549 and LLC) were treated with conditioned medium from M0, M2 or CB-treated M2 macrophages. Then, the supernatants of the treated lung cancer cells were used to treat HUVECs. As shown in Figs. S2 and S3, the tube formation ability of HUVECs was significantly enhanced in the M2 group compared with the M0 group, and the tube formation ability was attenuated in the M2 + CB group compared with the M2 group.

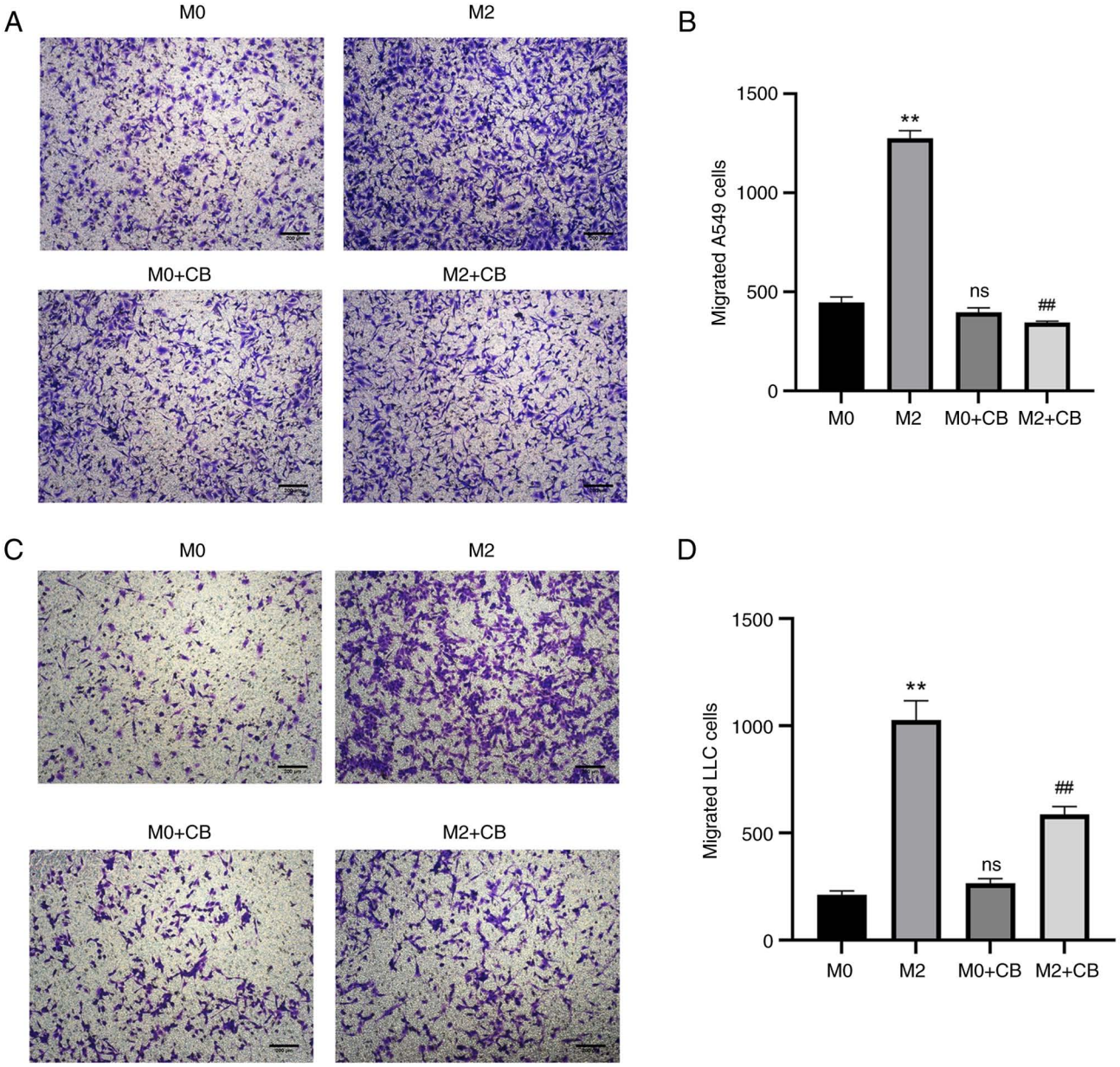

Figure 7. Effect of CB on invasion of A549 and LLC cells on conditioned medium culture of macrophages in different polarization states. (A and B) Invasive ability of A549 cells with different treatments was evaluated by Transwell invasion assay. (C and D) Invasive ability of LLC cells with different treatments was evaluated by Transwell invasion assay (n=3). **P<0.01 compared with M0 group; $^{\#\#}$P<0.01 compared with M2 group. CB, cinobufagin; ns, not statistically significant compared with M0 group.

Effects of RSG on cell viability and PPARγ and MARCO expression in macrophages with different polarization states. Research has found that PPARγ can regulate the expression of the M2 macrophage-related factor, Arg-1 (25). Additionally, PPARγ can promote the progression of colon cancer cells and the growth of mouse tumors by affecting M2 polarization. RSG is an agonist of PPARγ. As demonstrated in Fig. 8A, RSG concentrations ranging from 0.1-10 μM had no effect on M0 macrophage viability. PPARγ mRNA expression in M2 macrophages was higher than that in M0 macrophages, which was significantly downregulated by CB treatment but not by RSG treatment (Fig. 8B). Additionally, CB treatment downregulated PPARγ mRNA expression in RSG-treated M2 macrophages (Fig. 8B). The nuclear translocation of PPARγ was enhanced in M2 macrophages compared with M0 macrophages. CB treatment decreased PPARγ expression in the nucleus, whereas RSG treatment increased PPARγ expression in the nucleus of M2 macrophages. Furthermore, CB treatment reversed the RSG-induced increase in nuclear expression of PPARγ in M2 macrophages (Fig. 8C). MARCO belongs to the class A scavenger receptor molecules. Research has revealed that macrophages express MARCO extensively on their surface, and MARCO^{+} TAMs in the TME tend to exhibit the M2 phenotype (40). In the present study, the expression of MARCO was elevated in M2 macrophages compared with M0 macrophages. CB treatment decreased MARCO expression in the nucleus, while RSG treatment increased MARCO expression in M2 macrophages. Furthermore, RSG treatment partially restored the CB-induced decrease in MARCO expression in M2 macrophages (Fig. 8D). These results indicated that CB

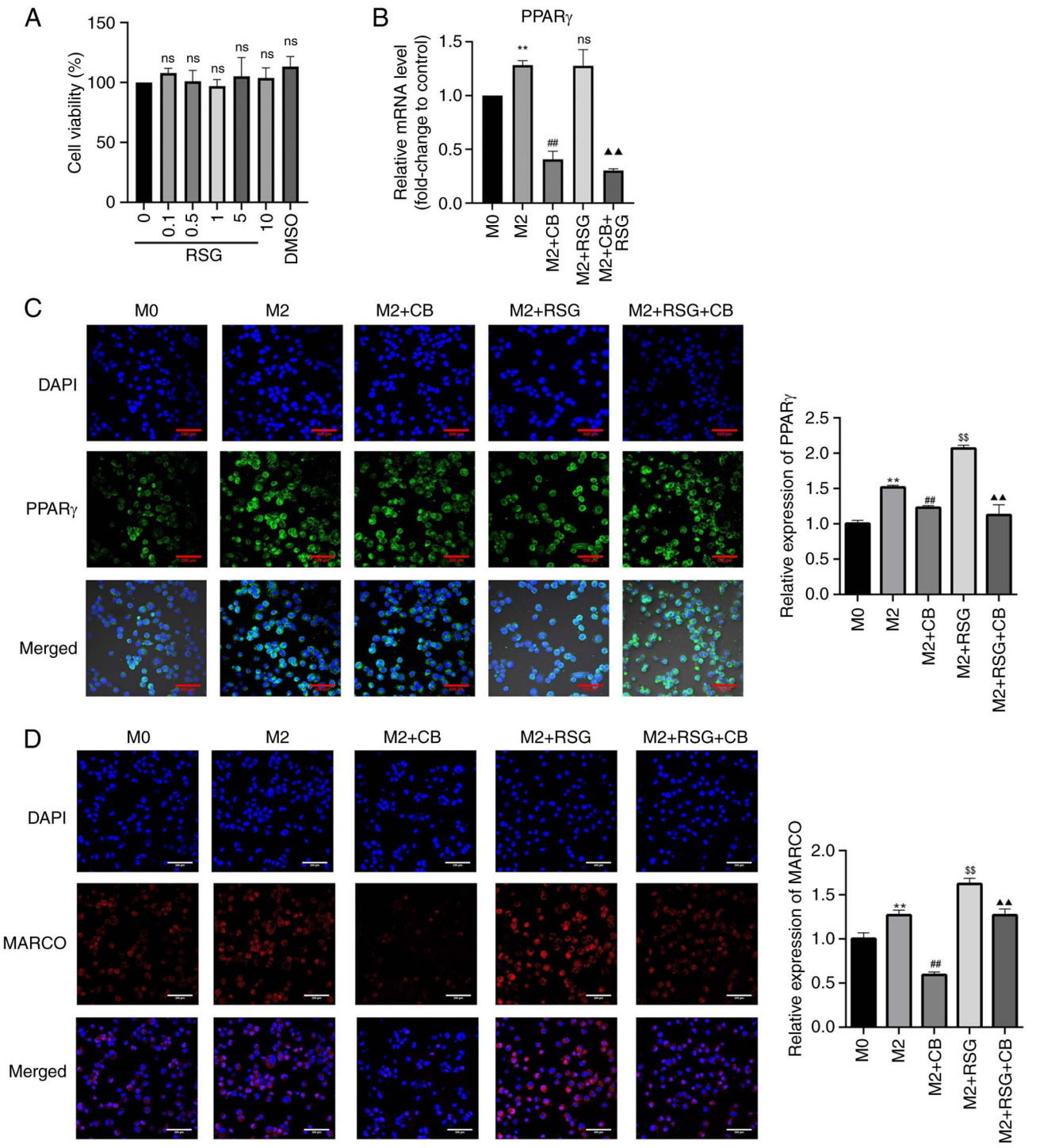

Figure 8. Effects of RSG on the cell viability, PPARγ and MARCO expression in macrophages with different polarization states. (A) Effects of different concentrations of RSG on cell viability of M0 macrophages were determined by MTT assay. (B) The mRNA expression of PPARγ in different treatment groups were determined by reverse transcription-quantitative PCR. (C) Expression and location of PPARγ in cells with different treatments were evaluated by IF staining. (D) Expression and location of MARCO in cells with different treatments were evaluated by IF staining (n=3). **P<0.01 compared with M0 group; $^{\#\#}$P<0.01 and $^{\$\$}$P<0.01 compared with M2 group; $^{\blacktriangle\blacktriangle}$P<0.01 compared with M2 + RSG group. RSG, rosiglitazone; PPARγ, peroxisome proliferator-activated receptor γ; MARCO, macrophage receptor with collagenous structure; IF, immunofluorescence; ns, not statistically significant compared with 0 μM RSG group.

treatment significantly downregulated PPARγ mRNA expression and nuclear translocation in M2 macrophages, whereas RSG treatment had opposite effects, with CB reversing the RSG-induced increase in PPARγ expression; additionally, CB reduced MARCO expression in M2 macrophages, while RSG partially restored CB-induced MARCO downregulation.

Effects of CB on the expression of macrophage polarization-related proteins. As shown in Fig. 9A, the effects of CB on macrophage polarization-related proteins were assessed. Arg-1 protein expression was upregulated in M2 macrophages compared with M0 macrophages. CB treatment repressed Arg-1 protein expression, whereas RSG elevated Arg-1 protein

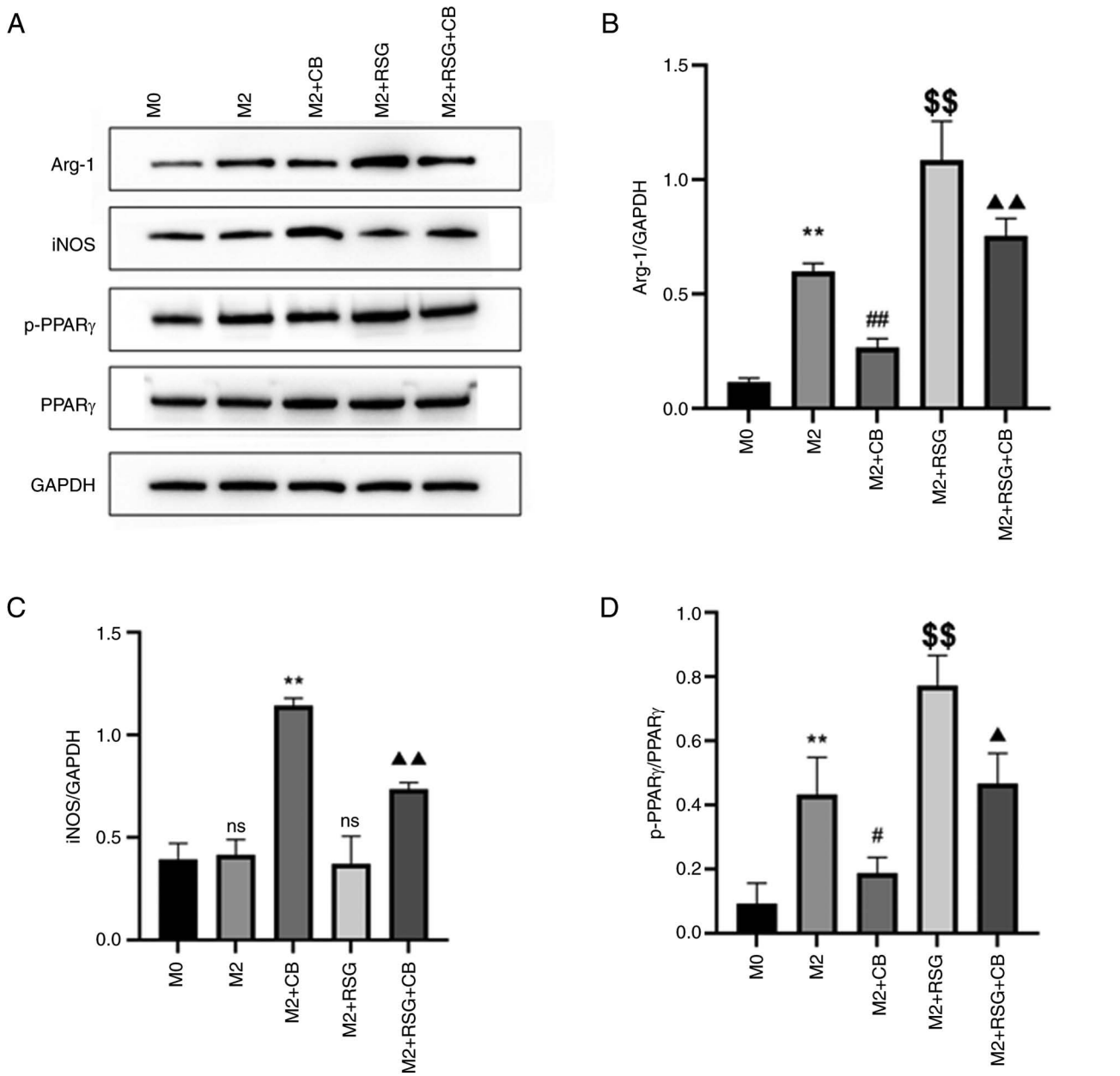

Figure 9. Effects of CB on the expression of macrophage polarization-related proteins. (A) Gel blots showing protein expression of Arg-1, iNOS, p-PPARγ and PPARγ in cells with different treatment groups. (B-D) Quantification of (B) Arg-1, (C) iNOS and (D) p-PPARγ based on the western blot assay (n=3). **P<0.01 compared with M0 group; $^{\#}$P<0.05, $^{\#\#}$P<0.01 and $^{\$\$}$P<0.01 compared with M2 group; $^{\blacktriangle}$P<0.05 and $^{\blacktriangle\blacktriangle}$P<0.01 compared with M2 + RSG group. CB, cinobufagin; Arg-1, arginase 1; iNOS, inducible nitric oxide synthase; p-, phosphorylated; PPARγ, peroxisome proliferator-activated receptor γ; RSG, rosiglitazone; ns from M2 group, not statistically significant compared with M0 group; ns from M2 + RSG group, not statistically significant compared with M2 group.

expression in M2 macrophages (Fig. 9A and B). Furthermore, CB treatment attenuated the RSG-induced increase in Arg-1 protein expression in M2 macrophages (Fig. 9A and B). No difference in iNOS protein expression between M0 and M2 macrophages was observed (Fig. 9A-C). CB treatment increased iNOS protein expression, while RSG had no effect on iNOS expression in M2 macrophages (Fig. 9A and C). Additionally, RSG treatment partially mitigated the CB-induced increase in iNOS expression in M2 macrophages (Fig. 9A and C). p-PPARγ expression was upregulated in M2 macrophages compared with M0 macrophages. CB treatment repressed p-PPARγ protein expression, while RSG elevated p-PPARγ protein expression in M2 macrophages (Fig. 9A and D). Furthermore, CB treatment attenuated the RSG-induced increase in p-PPARγ protein expression in M2 macrophages (Fig. 9A and D). These results revealed that in M2 macrophages, CB treatment decreased Arg-1 and p-PPARγ protein expression while increasing iNOS protein expression; conversely, RSG treatment increased Arg-1 and p-PPARγ expression without affecting iNOS, with RSG partially reversing the CB-induced effects on these proteins.

Effects of CB-treated macrophage-conditioned medium on EMT-related protein expression in lung cancer cells. EMT is the process by which polarized epithelial cells transform into mesenchymal-like cells. During this transformation, cell surface epithelial markers such as E-cadherin and desmoplakin are downregulated, while mesenchymal markers such

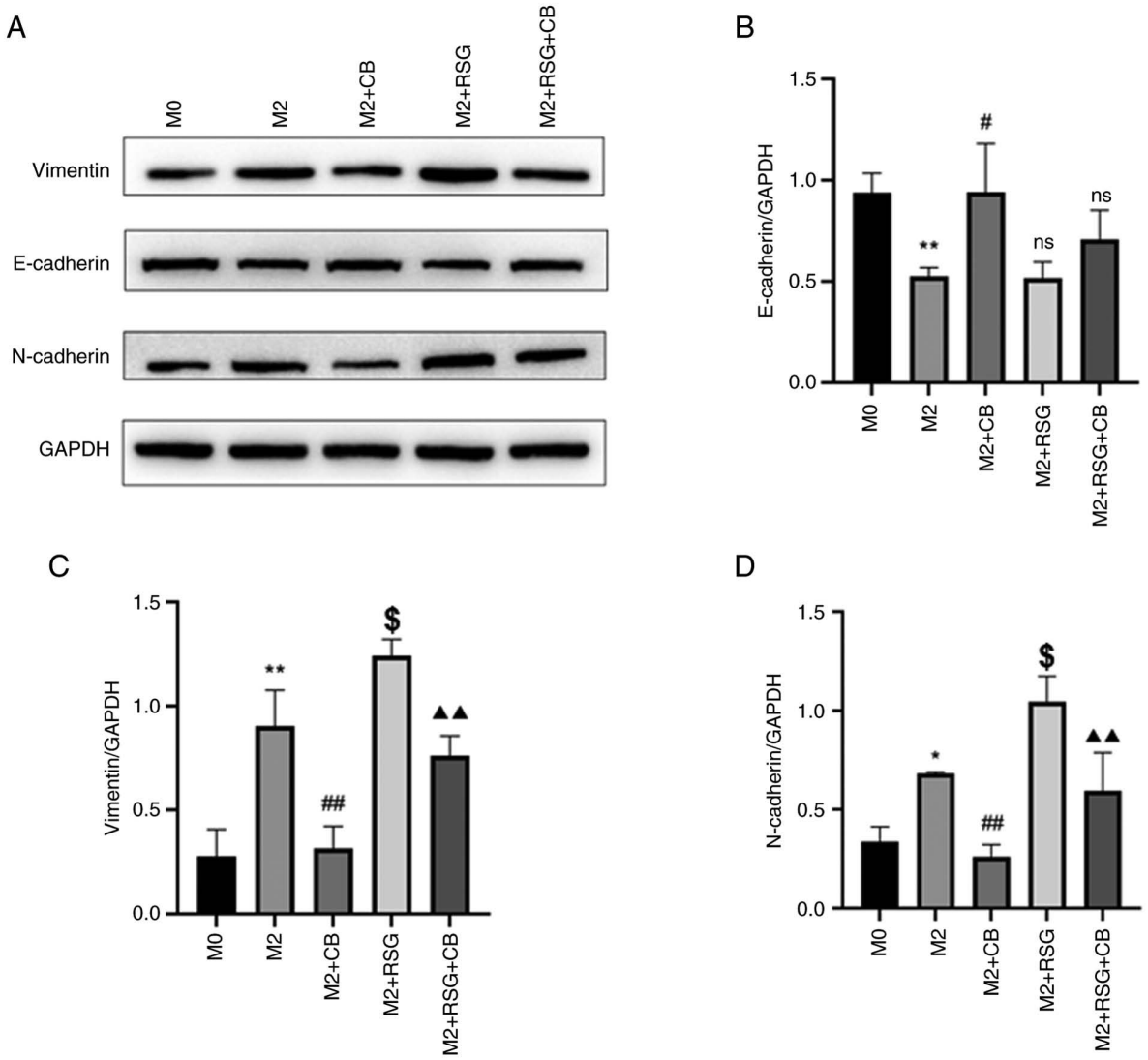

Figure 10. Conditioned medium culture of CB-treated macrophages in different polarization states on epithelial-mesenchymal transition-related proteins expression of lung cancer cells. (A) Gel blots showing protein expression of vimentin, E-cadherin and N-cadherin in A549 cells with different treatment groups. (B-D) Quantification of (B) E-cadherin, (C) vimentin and (D) N-cadherin based on the western blot assay (n=3). *P<0.05, **P<0.01 compared with M0 group; $^{\#}$P<0.05, $^{\#\#}$P<0.01 and $^{\$}$P<0.05 compared with M2 group; $^{\blacktriangle\blacktriangle}$P<0.01 compared with M2 + RSG group. CB, cinobufagin; RSG, rosiglitazone; ns from M2 + RSG group, not statistically significant compared with M2 group; ns from M2 + RSG + CB group, not statistically significant compared with M2 + RSG group.

as N-cadherin and vimentin are upregulated, resulting in the loss of cell adhesion and apical-basal polarity, which promotes tumor progression and metastasis (41). As demonstrated in Fig. 10A, the effects of CB on EMT-related proteins in A549 lung cancer cells were assessed using western blotting. E-cadherin was downregulated in A549 cells treated with M2 macrophage-conditioned medium compared with M0 macrophage-condition medium (Fig. 10A and B). The E-cadherin protein level was increased in A549 cells cultured with CB-treated M2 macrophage-conditioned medium compared with M2 macrophage-conditioned medium, while RSG-treated M2 macrophage-conditioned medium had no effect on E-cadherin expression in A549 cells compared with M2 macrophage-conditioned medium (Fig. 10A and B).

Vimentin and N-cadherin were upregulated in A549 cells treated M2 macrophage-conditioned medium compared with M0 macrophage-condition medium (Fig. 10A, C and D). The vimentin and N-cadherin protein levels were decreased in A549 cells cultured with CB-treated with M2 macrophage-conditioned medium compared with M2 macrophage-conditioned medium, while RSG-treated M2 macrophage-conditioned medium increased vimentin and N-cadherin protein levels in A549 cells compared with M2 macrophage-conditioned medium (Fig. 10A, C and D). Furthermore, the RSG-mediated effects on vimentin and N-cadherin expression in A549 cells were attenuated by CB treatment (Fig. 10A, C and D). The results indicated that in A549 lung cancer cells, treatment with M2 macrophage-conditioned medium downregulated E-cadherin and upregulated vimentin and N-cadherin levels, effects attenuated by CB treatment but exacerbated by RSG treatment, indicating modulation of EMT-related protein expression.

Effects of CB and DDP on in vivo tumor growth. The effects of CB on *in vivo* tumor growth were further examined using a nude mice xenograft model. As revealed in Fig. 11A-C, both

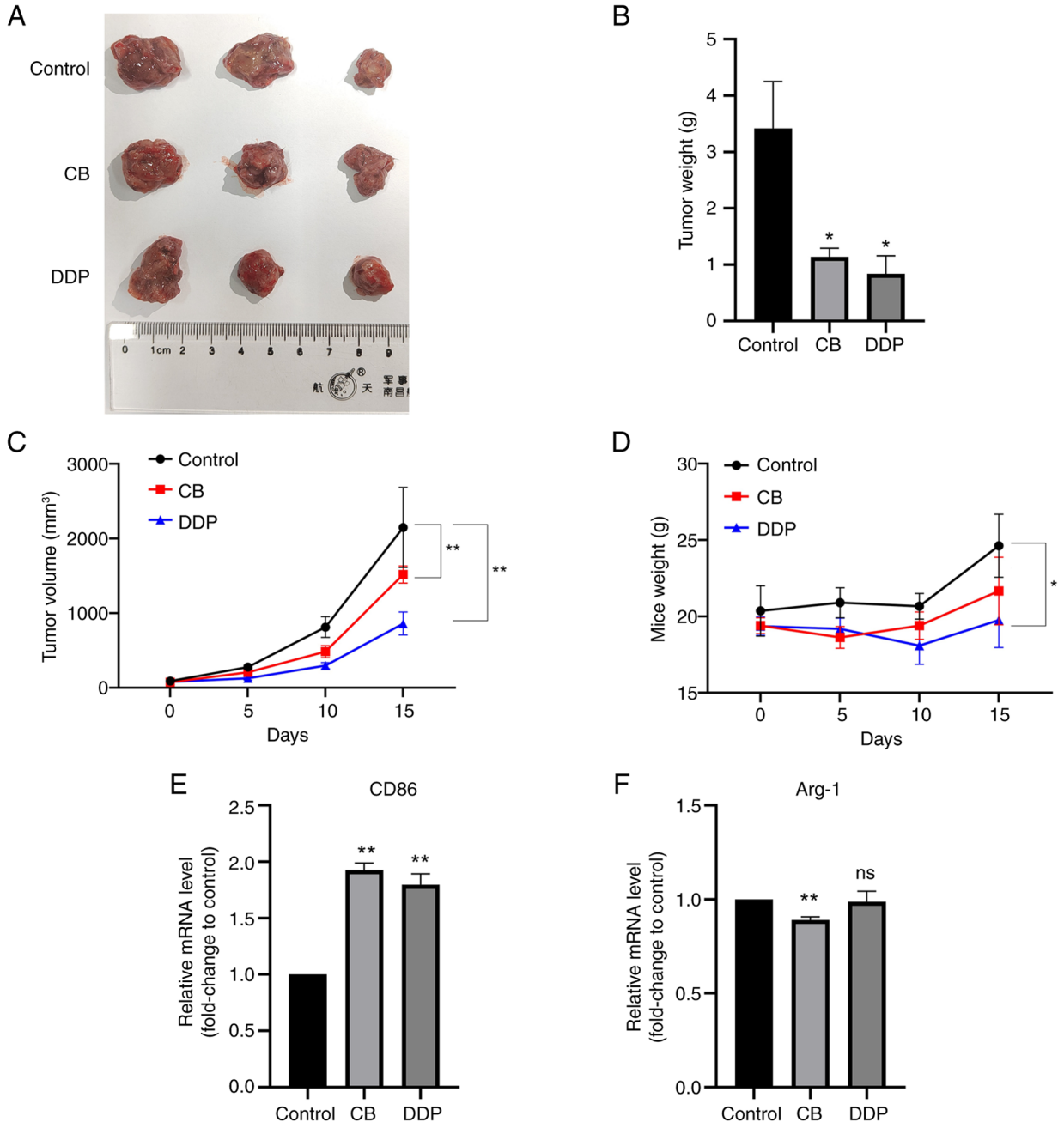

Figure 11. Effects of CB and DDP on the *in vivo* tumor growth. (A) Representative images of dissected tumor tissues. (B) Tumor weight of the mice received different treatments. (C) Tumor growth (volume) of the mice received different treatments. (D) Body weight of the mice with different treatments. (E) The mRNA expression of CD86 in the tumor tissues with different treatments. (F) The mRNA expression of Arg-1 in the tumor tissues with different treatments (n=6). *P<0.05, **P<0.01 compared with control group. CB, cinobufagin; DDP, cisplatin; Arg-1, arginase 1; ns, not statistically significant compared with control group.

DDP and CB treatments inhibited the *in vivo* tumor growth of LLC cells. However, DDP, but not CB, reduced the body weight of the nude mice. Additionally, both CB and DDP treatments significantly upregulated CD86 mRNA expression in the tumor tissues (Fig. 11E). However, CB, but not DDP, downregulated Arg-1 expression in the tumor tissues compared with the control group (Fig. 11F). These results indicated that both CB and DDP treatments effectively suppressed LLC tumor growth and increased CD86 mRNA expression in tumor tissues, with DDP additionally reducing body weight and CB uniquely downregulating Arg-1 expression compared with controls.

Discussion

Lung cancer is one of the most common malignant tumors worldwide, with its incidence and mortality rates increasing annually (1). In the TME, interactions between tumor and immune cells directly influence tumor progression (10). TAMs have a dual regulatory role in lung cancer malignancy, among which the quantity, activity and function of M2 macrophages are closely related to tumor progression (10,14). HuaChanSu injection has been used for treating lung cancer clinically (29). Furthermore, a HuaChanSu injection and DDP combination improves efficacy in the treatment of advanced

NSCLC, with a higher quality of life for patients and fewer adverse reactions (7). Bufadienolide glycosides, including CB and bufalin, are the main antitumor active ingredients in HuaChanSu injection, but their exact mechanisms of action remain unclear (42). At present, most research on the antitumor mechanism of CB focus on inhibiting tumor cell proliferation and promoting apoptosis, with fewer studies on the molecular mechanisms of tumor invasion and migration. Therefore, based on the significant clinical antitumor efficacy of HuaChanSu injection, the present study aimed to reveal the influence and mechanism of action of its effective active ingredient, CB, on the polarization of TAMs, to provide a basis for further exploration of the pharmacological actions and clinical applications of CB.

In the complex TME, TAMs interact with the TME, undergo metabolic changes and alter the anticancer phenotype of early M1-TAMs (43). Typically, in the early stages of tumor development, M1-like TAMs predominate the TME and inhibit tumor growth by secreting certain inflammatory factors (44). As cancer progresses, late-stage M2-like TAMs begin to dominate the TME, promoting angiogenesis and aiding in tumor cell dissemination and metastasis, thus exhibiting pro-tumor effects (40). THP-1 monocytes differentiate into macrophages when induced by PMA, leading to changes in cell morphology and surface markers (45). Exposure to the Th1 cytokine, IFN-γ, induces differentiation into M1-type macrophages, while exposure to the Th2 cytokine, IL-4, induces differentiation into M2-type macrophages, which is typically accompanied by changes in cell surface marker expression (46). Therefore, the widely used PMA was adopted in the present study to induce the differentiation of THP-1 cells into M0 macrophages, which were then separately induced into M1 or M2 macrophage models using human IFN-γ or IL-4, respectively. The results demonstrated that after PMA stimulation, the cells enlarged and adhered to the wall, and the mRNA levels of the M0 macrophage surface marker CD86 increased, indicating the successful induction of M0 macrophages. Under IFN-γ stimulation, the surface expression of the M1 polarization marker CD86 increased, accompanied by secretion of high levels of pro-inflammatory cytokines. After IL-4 stimulation, the levels of CD206 increased. These results were consistent with previous studies (36,47) indicating the successful replication of macrophage models with different polarization phenotypes.

Pharmacological studies have demonstrated that HuaChanSu injection has significant antitumor, analgesic and immune-enhancing effects, and is commonly used clinically to treat primary liver cancer, lung cancer, CRC and other diseases (48). CB possesses antitumor, analgesic, cardiotonic and local anesthetic effects, but it also has certain toxicities, particularly cardiac toxicity (49,50). In the present study, the MTT method was used to assess the effects of different concentrations (0, 10, 15, 20, 25, 30, 35, 40 and 50 ng/ml) of CB on the viability of M0 macrophages. The results indicated that, as the drug concentration increased the cell viability gradually decreased, and when the concentration was <30 ng/ml, the viability of M0 cells was >80%. In addition, to further evaluate the safety of CB, the viability of BEAS-2B cells was assessed. The results showed that when the concentration was <30 ng/ml, CB had no clear toxic effect on BEAS-2B cells. Ultimately, 25 ng/ml was selected as the CB concentration for subsequent experiments.

The balance between M1 and M2 macrophages will affect the overall antitumor or pro-tumor effects of macrophages. Therefore, maintaining the M1/M2 macrophage balance in the body has become an important strategy for antitumor therapy. At present, immunotherapy based on macrophages aims to reduce the proportion of M2 macrophages or repolarize M2 into M1 macrophages to inhibit tumor invasion and metastasis (51). Traditional Chinese Medicine and its active ingredients can regulate the balance of M1/M2 macrophages. The active ingredient, β-elemene, in *Curcuma aromatica* can inhibit the migration, invasion and EMT of LLC cells induced by M2 macrophage-conditioned medium (52). β-elemene downregulates Arg-1 and upregulates iNOS expression, suggesting that its effect on tumor cell invasion and migration may be achieved through regulating the balance of M1/M2 macrophages (52). Consistently, the results of the present study suggested that CB is key in maintaining the M1/M2 macrophage balance, promoting M1 polarization and inhibiting M2 polarization.

Macrophages participate in various stages of tumor metastasis, in which M2 macrophages can assist tumor cells in penetrating blood vessels and entering the bloodstream in the form of circulating tumor cells, thus facilitating the subsequent settlement of tumor cells (53). Additionally, the infiltration density of M2 macrophages is correlated with the generation of microvessels within tumors and is negatively correlated with patient survival (54). In the present study, M2 macrophage-conditioned medium was prepared and separately cultured with the A549 and LLC lung cancer cell lines, to observe the effects on the invasion, migration and angiogenic abilities of these cells. The results showed that M2 macrophage-conditioned medium promoted the invasion, migration and angiogenesis of A549 and LLC cells, while pre-treatment with CB significantly inhibited the invasion, migration and angiogenesis of these cells in M2 macrophage-conditioned medium. A study has shown that M2-like TAMs can induce EMT through the secretion of TGF-β1, activating the TGF-β signaling pathway via Smad-dependent or Smad-independent signaling pathways (55). In the present study, the expression levels of the EMT-related proteins, vimentin, E-cadherin and N-cadherin, in A549 lung cancer cells were also examined. The A549 cells cultured in M2 macrophage-conditioned medium exhibited a significant increase in vimentin and N-cadherin levels and a decrease in E-cadherin levels, supporting the notion that M2 macrophages promote lung cancer cell progression. When the A549 cells were cultured in M2 macrophage-conditioned medium pre-treated with CB, the vimentin and N-cadherin levels significantly decreased, while E-cadherin expression increased. These results suggested that the inhibition of lung cancer cell invasion and migration by CB may be achieved through regulating macrophage polarization to influence EMT-related protein expression in lung cancer cells.

Research has demonstrated that MARCO is extensively expressed on the surface of macrophages, and MARCO$^+$TAMs in the TME tend to exhibit the M2 phenotype (40). In a mouse glioblastoma model, peritoneal macrophages overexpressing PPARγ increased the

transcription levels of MARCO, driving the formation of M2 macrophages (56). Whether the CB-inhibited M2 polarization is related to MARCO expression has not, to the best of our knowledge, been reported. In the present study, IF techniques were used to detect MARCO expression in macrophages. The results demonstrated that the average fluorescence intensity of MARCO in M2 macrophages was higher than that in M0 macrophages; however, after pretreatment with CB, the average fluorescence intensity of MARCO decreased, suggesting that CB downregulated MARCO expression on the surface of M2 macrophages.

The present study demonstrated that there was no significant change in the PPARγ mRNA level in M2 macrophages following RSG stimulation. It was hypothesized that PPARγ might exert its effects through self-phosphorylation and/or nuclear translocation. The experimental results showed that the phosphorylation level of PPARγ in M2 macrophages significantly increased after RSG stimulation, and a large amount of PPARγ was translocated to the nucleus. Collectively, these results indicated that the transcription factor, PPARγ, can promote M2 polarization through phosphorylation and nuclear translocation. In the present study, to verify whether the observed CB-inhibited M2 polarization was related to the regulation of PPARγ, macrophages were pretreated with CB, and after RSG stimulation, CB partially inhibited the phosphorylation and nuclear translocation of PPARγ in M2 macrophages. These results suggested that CB can prevent PPARγ activation and thus affect macrophage polarization.

In the present study, to further clarify whether the impact of CB on NSCLC progression was related to PPARγ, RSG was used to treat and collect macrophage-conditioned medium for culturing A549 cells. Upon examination, it was found that RSG pre-treated macrophage-conditioned medium induced a high expression of vimentin and N-cadherin in A549 cells, while E-cadherin expression remained unchanged; meanwhile, CB reversed these changes. These results suggested that CB may inhibit M2 polarization by targeting PPARγ in M2 macrophages, thereby affecting lung cancer cell progression.

However, the present study still has certain limitations and further research is needed on the mechanism by which CB inhibits lung cancer invasion and migration. Further research is planned in the following three areas. First, the present study lacked verification at the *in vivo* animal level regarding whether CB inhibits lung cancer invasion and migration by affecting macrophage polarization. The present study preliminarily demonstrated that CB inhibited LLC xenograft growth in mice and modulated the gene expression levels of the M1 macrophage surface marker, CD86, and the M2 macrophage surface marker, Arg-1, in tumor tissues, but detailed experimental research is still ongoing. Second, TAM phenotype and function in the TME are also influenced by metabolic reprogramming, including glutamine, glucose and fatty acid metabolisms. Therefore, it remains to be further clarified whether CB regulates macrophage polarization by modulating metabolism. Third, communication between TAMs and lung cancer cells can also be achieved through exosomes. Therefore, exosomes could be used as carriers for anticancer drug delivery systems. Compared with other types of macrophages, M1 macrophages have stronger phagocytic capacity for loading anticancer drug nanoparticles (57). Using M1 macrophage exosomes as carriers and utilizing Traditional Chinese Medicine nanotechnology for the precise targeting of tumor sites may improve anticancer effects. Fourth, the detailed interactions between MARCO and PPARγ were not fully elucidated in the present work, which should be further deciphered. Fifth, the present study primarily focused on the effects of CB, with limited exploration of alternative treatments or combination therapies. Considering the complex nature of cancer and macrophage biology, comparative studies with other treatments or synergistic combinations may provide valuable insights into potential therapeutic strategies. Furthermore, the expression of CD86 and Arg-1 in tumor tissues was detected only the mRNA level, and further studies should determine the protein levels of CD86 and Arg-1 in the tumor tissues to consolidate the findings.

In summary, the inhibition of NSCLC invasion, migration and angiogenesis by CB potentially operates through several mechanisms: Suppressing PPARγ phosphorylation and nuclear translocation, lowering MARCO expression, hindering M2 macrophage polarization, enhancing secretion of inflammatory factors linked to M1 macrophages, balancing the M1/M2 macrophage ratios, ameliorating NSCLC TME immunosuppression and impacting EMT-related protein expression levels.

Acknowledgements

Not applicable.

Funding

The present study was supported by the National Nature Science Foundation of China (grant no. 81803863), the Programs for Science and Technology Development of Henan (grant no. 232102311111) and the Henan Provincial College Youth Key Teacher Training Program (grant no. 2020GGJS103).

Availability of data and materials

The data generated in the present study may be requested from the corresponding author.

Authors' contributions

YS, YL and XM conceived and designed the experiments. YS, YL, XM, JX, LF and JG performed the experiments. HX XZ, HY, XH and YF analyzed the data. HY, XH and YF contributed to the provision of reagents/materials/analysis tools. YS, YL and XM confirm the authenticity of all the raw data. All authors drafted and edited the manuscript. All authors read and approved the final version of the manuscript.

Ethics approval and consent to participate

The present study was approved (approval no. IACUC-202302006) by the animal Ethics Committee of Henan University of Chinese Medicine (Zhengzhou, China).

Patient consent for publication

Not applicable.

Competing interests

The authors declare that they have no competing interests.

References

1. Kratzer TB, Bandi P, Freedman ND, Smith RA, Travis WD, Jemal A and Siegel RL: Lung cancer statistics, 2023. Cancer 130: 1330-1348, 2023.
2. Lee E and Kazerooni EA: Lung cancer screening. Semin Respir Crit Care Med 43: 839-850, 2022.
3. Schabath MB and Cote ML: Cancer progress and priorities: Lung cancer. Cancer Epidemiol Biomarkers Prev 28: 1563-1579, 2019.
4. Zheng M: Classification and pathology of lung cancer. Surg Oncol Clin N Am 25: 447-468, 2016.
5. Rodriguez-Canales J, Parra-Cuentas E and Wistuba II: Diagnosis and molecular classification of lung cancer. Cancer Treat Res 170: 25-46, 2016.
6. Srivastava S, Mohanty A, Nam A, Singhal S and Salgia R: Chemokines and NSCLC: Emerging role in prognosis, heterogeneity, and therapeutics. Semin Cancer Biol 86: 233-246, 2022.
7. Duma N, Santana-Davila R and Molina JR: Non-small cell lung cancer: Epidemiology, screening, diagnosis, and treatment. Mayo Clin Proc 94: 1623-1640, 2019.
8. Miller M and Hanna N: Advances in systemic therapy for non-small cell lung cancer. BMJ 375: n2363, 2021.
9. Osmani L, Askin F, Gabrielson E and Li QK: Current WHO guidelines and the critical role of immunohistochemical markers in the subclassification of non-small cell lung carcinoma (NSCLC): Moving from targeted therapy to immunotherapy. Semin Cancer Biol 52: 103-109, 2018.
10. Wang Y, Chen R, Wa Y, Ding S, Yang Y, Liao J, Tong L and Xiao G: Tumor immune microenvironment and immunotherapy in brain metastasis from non-small cell lung cancer. Front Immunol 13: 829451, 2022.
11. Cascone T, Fradette J, Pradhan M and Gibbons DL: Tumor immunology and immunotherapy of non-small-cell lung cancer. Cold Spring Harb Perspect Med 12: a037895, 2022.
12. Sivori S, Pende D, Quatrini L, Pietra G, Della Chiesa M, Vacca P, Tumino N, Moretta F, Mingari MC, Locatelli F and Moretta L: NK cells and ILCs in tumor immunotherapy. Mol Aspects Med 80: 100870, 2021.
13. Herbst RS, Morgensztern D and Boshoff C: The biology and management of non-small cell lung cancer. Nature 553: 446-454, 2018.
14. Cheng D, Ge K, Yao X, Wang B, Chen R, Zhao W, Fang C and Ji M: Tumor-associated macrophages mediate resistance of EGFR-TKIs in non-small cell lung cancer: Mechanisms and prospects. Front Immunol 14: 1209947, 2023.
15. Sedighzadeh SS, Khoshbin AP, Razi S, Keshavarz-Fathi M and Rezaei N: A narrative review of tumor-associated macrophages in lung cancer: Regulation of macrophage polarization and therapeutic implications. Transl Lung Cancer Res 10: 1889-1916, 2021.
16. Genova C, Dellepiane C, Carrega P, Sommariva S, Ferlazzo G, Pronzato P, Gangemi R, Filaci G, Coco S and Croce M: Therapeutic implications of tumor microenvironment in lung cancer: Focus on immune checkpoint blockade. Front Immunol 12: 799455, 2022.
17. Yuan A, Hsiao YJ, Chen HY, Chen HW, Ho CC, Chen YY, Liu YC, Hong TH, Yu SL, Chen JJ and Yang PC: Opposite effects of M1 and M2 macrophage subtypes on lung cancer progression. Sci Rep 5: 14273, 2015.
18. Sumitomo R, Hirai T, Fujita M, Murakami H, Otake Y and Huang CL: M2 tumor-associated macrophages promote tumor progression in non-small-cell lung cancer. Exp Ther Med 18: 4490-4498, 2019.
19. Hu JM, Liu K, Liu JH, Jiang XL, Wang XL, Yang L, Chen YZ, Liu CX, Li SG, Cui XB, *et al*: The increased number of tumor-associated macrophage is associated with overexpression of VEGF-C, plays an important role in Kazakh ESCC invasion and metastasis. Exp Mol Pathol 102: 15-21, 2017.
20. Frezzetti D, Gallo M, Maiello MR, D'Alessio A, Esposito C, Chicchinelli N, Normanno N and De Luca A: VEGF as a potential target in lung cancer. Expert Opin Ther Targets 21: 959-966, 2017.
21. Zeni E, Mazzetti L, Miotto D, Lo Cascio N, Maestrelli P, Querzoli P, Pedriali M, De Rosa E, Fabbri LM, Mapp CE and Boschetto P: Macrophage expression of interleukin-10 is a prognostic factor in nonsmall cell lung cancer. Eur Respir J 30: 627-632, 2007.
22. Vahl JM, Friedrich J, Mittler S, Trump S, Heim L, Kachler K, Balabko L, Fuhrich N, Geppert CI, Trufa DI, *et al*: Interleukin-10-regulated tumour tolerance in non-small cell lung cancer. Br J Cancer 117: 1644-1655, 2017.
23. Maltarollo VG, Kronenberger T, Windshugel B, Wrenger C, Trossini GHG and Honorio KM: Advances and challenges in drug design of PPARδ ligands. Curr Drug Targets 19: 144-154, 2018.
24. Tontonoz P and Spiegelman BM: Fat and beyond: The diverse biology of PPARgamma. Annu Rev Biochem 77: 289-312, 2008.
25. Gallardo-Soler A, Gómez-Nieto C, Campo ML, Marathe C, Tontonoz P, Castrillo A and Corraliza I: Arginase I induction by modified lipoproteins in macrophages: A peroxisome proliferator-activated receptor-gamma/delta-mediated effect that links lipid metabolism and immunity. Mol Endocrinol 22: 1394-1402, 2008.
26. Huang JT, Welch JS, Ricote M, Binder CJ, Willson TM, Kelly C, Witztum JL, Funk CD, Conrad D and Glass CK: Interleukin-4-dependent production of PPAR-gamma ligands in macrophages by 12/15-lipoxygenase. Nature 400: 378-382, 1999.
27. Bu ZJ, Wan SR, Steinmann P, Yin ZT, Tan JP, Li WX, Tang ZY, Jiang S, Ye MM and Xu JY: Effectiveness and safety of Chinese herbal injections combined with SOX chemotherapy regimens for advanced gastric cancer: A Bayesian network meta-analysis. J Cancer 15: 889-907, 2024.
28. Tarasiuk A, Mirocha G and Fichna J: Current status of complementary and alternative medicine interventions in the management of pancreatic cancer-an overview. Curr Treat Options Oncol 24: 1852-1869, 2023.
29. Xu YF, Chen YR, Bu FL, Huang YB, Sun YX, Li CY, Sellick J, Liu JP, Qin DM and Liu ZL: Chinese herbal injections versus intrapleural cisplatin for lung cancer patients with malignant pleural effusion: A Bayesian network meta-analysis of randomized controlled trials. Front Oncol 12: 942941, 2022.
30. Tan X, Liang X, Xi J, Guo S, Meng M, Chen X and Li Y: Clinical efficacy and safety of Huachansu injection combination with platinum-based chemotherapy for advanced non-small cell lung cancer: A systematic review and meta-analysis of randomized controlled trials. Medicine (Baltimore) 100: e27161, 2021.
31. He K, Wang GX, Zhao LN, Cui XF, Su XB, Shi Y, Xie TP, Hou SW and Han ZG: Cinobufagin is a selective anti-cancer agent against tumors with EGFR amplification and PTEN deletion. Front Pharmacol 12: 775602, 2021.
32. Bai Y, Wang X, Cai M, Ma C, Xiang Y, Hu W, Zhou B, Zhao C, Dai X, Li X and Zhao H: Cinobufagin suppresses colorectal cancer growth via STAT3 pathway inhibition. Am J Cancer Res 11: 200-214, 2021.
33. Ma X, Suo Z, Ma X, Zhan C, Luo G and Song J: Cinobufagin inhibits tumor progression and reduces doxorubicin resistance by enhancing FOXO1-mediated transcription of FCGBP in osteosarcoma. J Ethnopharmacol 296: 115433, 2022.
34. Zhang L, Liang B, Xu H, Gong Y, Hu W, Jin Z, Wu X, Chen X, Li M, Shi L, *et al*: Cinobufagin induces FOXO1-regulated apoptosis, proliferation, migration, and invasion by inhibiting G9a in non-small-cell lung cancer A549 cells. J Ethnopharmacol 291: 115095, 2022.
35. Mantovani A, Sozzani S, Locati M, Allavena P and Sica A: Macrophage polarization: Tumor-associated macrophages as a paradigm for polarized M2 mononuclear phagocytes. Trends Immunol 23: 549-555, 2002.
36. Xu F, Cui WQ, Wei Y, Cui J, Qiu J, Hu LL, Gong WY, Dong JC and Liu BJ: Astragaloside IV inhibits lung cancer progression and metastasis by modulating macrophage polarization through AMPK signaling. J Exp Clin Cancer Res 37: 207, 2018.
37. Livak KJ and Schmittgen TD: Analysis of relative gene expression data using real-time quantitative PCR and the 2(-Delta Delta C(T)) method. Methods 25: 402-408, 2001.
38. Niu J, Wang J, Zhang Q, Zou Z and Ding Y: Cinobufagin-induced DNA damage response activates G2/M checkpoint and apoptosis to cause selective cytotoxicity in cancer cells. Cancer Cell Int 21: 446, 2021.

39. Lu XS, Qiao YB, Li Y, Yang B, Chen MB and Xing CG: Preclinical study of cinobufagin as a promising anti-colorectal cancer agent. Oncotarget 8: 988-998, 2017.
40. Murray PJ, Allen JE, Biswas SK, Fisher EA, Gilroy DW, Goerdt S, Gordon S, Hamilton JA, Ivashkiv LB, Lawrence T, *et al*: Macrophage activation and polarization: Nomenclature and experimental guidelines. Immunity 41: 14-20, 2014.
41. Mittal V: Epithelial mesenchymal transition in tumor metastasis. Annu Rev Pathol 13: 395-412, 2018.
42. Qi F, Inagaki Y, Gao B, Cui X, Xu H, Kokudo N, Li A and Tang W: Bufalin and cinobufagin induce apoptosis of human hepatocellular carcinoma cells via Fas- and mitochondria-mediated pathways. Cancer Sci 102: 951-958, 2011.
43. Netea-Maier RT, Smit JWA and Netea MG: Metabolic changes in tumor cells and tumor-associated macrophages: A mutual relationship. Cancer Lett 413: 102-109, 2018.
44. Redente EF, Dwyer-Nield LD, Merrick DT, Raina K, Agarwal R, Pao W, Rice PL, Shroyer KR and Malkinson AM: Tumor progression stage and anatomical site regulate tumor-associated macrophage and bone marrow-derived monocyte polarization. Am J Pathol 176: 2972-2985, 2010.
45. Xue J, Fu C, Cong Z, Peng L, Peng Z, Chen T, Wang W, Jiang H, Wei Q and Qin C: Galectin-3 promotes caspase-independent cell death of HIV-1-infected macrophages. FEBS J 284: 97-113, 2017.
46. Genin M, Clement F, Fattaccioli A, Raes M and Michiels C: M1 and M2 macrophages derived from THP-1 cells differentially modulate the response of cancer cells to etoposide. BMC Cancer 15: 577, 2015.
47. Chen R, Lu X, Li Z, Sun Y, He Z and Li X: Dihydroartemisinin prevents progression and metastasis of head and neck squamous cell carcinoma by inhibiting polarization of macrophages in tumor microenvironment. Onco Targets Ther 13: 3375-3387, 2020.
48. Huang J, Chen F, Zhong Z, Tan HY, Wang N, Liu Y, Fang X, Yang T and Feng Y: Interpreting the pharmacological mechanisms of huachansu capsules on hepatocellular carcinoma through combining network pharmacology and experimental evaluation. Front Pharmacol 11: 414, 2020.
49. Dai CL, Zhang RJ, An P, Deng YQ, Rahman K and Zhang H: Cinobufagin: A promising therapeutic agent for cancer. J Pharm Pharmacol 75: 1141-1153, 2023.
50. Asrorov AM, Kayumov M, Mukhamedov N, Yashinov A, Mirakhmetova Z, Huang Y, Yili A, Aisa HA, Tashmukhamedov M, Salikhov S and Mirzaakhmedov S: Toad venom bufadienolides and bufotoxins: An updated review. Drug Dev Res 84: 815-838, 2023.
51. Li X, Bu W, Meng L, Liu X, Wang S, Jiang L, Ren M, Fan Y and Sun H: CXCL12/CXCR4 pathway orchestrates CSC-like properties by CAF recruited tumor associated macrophage in OSCC. Exp Cell Res 378: 131-138, 2019.
52. Schmall A, Al-Tamari HM, Herold S, Kampschulte M, Weigert A, Wietelmann A, Vipotnik N, Grimminger F, Seeger W, Pullamsetti SS and Savai R: Macrophage and cancer cell cross-talk via CCR2 and CX3CR1 is a fundamental mechanism driving lung cancer. Am J Respir Crit Care Med 191: 437-447, 2015.
53. Nakatsumi H, Matsumoto M and Nakayama KI: Noncanonical pathway for regulation of CCL2 expression by an mTORC1-FOXK1 axis promotes recruitment of tumor-associated macrophages. Cell Rep 21: 2471-2486, 2017.
54. Wu CY, Cherng JY, Yang YH, Lin CL, Kuan FC, Lin YY, Lin YS, Shu LH, Cheng YC, Liu HT, *et al*: Danshen improves survival of patients with advanced lung cancer and targeting the relationship between macrophages and lung cancer cells. Oncotarget 8: 90925-90947, 2017.
55. Fu XH, Li JP, Li XY, Tan Y, Zhao M, Zhang SF, Wu XD and Xu JG: M2-macrophage-derived exosomes promote meningioma progression through TGF-β signaling pathway. J Immunol Res 2022: 8326591, 2022.
56. Sa JK, Chang N, Lee HW, Cho HJ, Ceccarelli M, Cerulo L, Yin J, Kim SS, Caruso FP, Lee M, *et al*: Transcriptional regulatory networks of tumor-associated macrophages that drive malignancy in mesenchymal glioblastoma. Genome Biol 21: 216, 2020.
57. Yu J, Deng H and Xu Z: Targeting macrophage priming by polyphyllin VII triggers anti-tumor immunity via STING-governed cytotoxic T-cell infiltration in lung cancer. Sci Rep 10: 21360, 2020.